RevMexAA (Serie de Conferencias), **1**, 43-58 (1995)

HERBIG-HARO JETS AT OPTICAL, INFRARED AND MILLIMETER WAVELENGTHS

Bo Reipurth
European Southern Observatory Casilla 19001, Santiago 19, Chile
and
José Cernicharo
Centro Astronómico de Yebes Apartado 148, 19080 Guadalajara, Spain

RESUMEN

En esta revisión se resume una serie de aspectos de la investigación actual de los objetos Herbig-Haro (HH). Para conseguir un conocimiento más completo sobre esos flujos se hace hincapié en que es necesario combinar observaciones en longitudes de onda ópticas, infrarrojas y milimétricas. Se revisa lo que actualmente se conoce sobre el chorro del sistema HH 46/47, discutiendo, además, la relación entre los chorros HH y los flujos moleculares, haciendo un énfasis especial en el sistema HH 111. Hoy día se conoce que los flujos HH pueden tener dimensiones mucho mayores que las que con anterioridad habían sido estimadas, lo que incrementa la posibilidad de que podamos presenciar la colisión de un chorro con un obstáculo de material denso, como parece que ocurre en un caso identificado recientemente. Finalmente, se describe el papel que desempeñan tanto las imágenes como la espectroscopía infrarroja en la investigación de los objetos HH.

ABSTRACT

This review summarizes a number of aspects of observational Herbig-Haro research as they presently stand. It is emphasized that for a more complete understanding of these flow phenomena one must combine observations at optical, infrared and mm wavelengths. Our current knowledge of the HH 46/47 jet complex is reviewed, and the relation between Herbig-Haro jets and molecular outflows is discussed with special reference to the HH 111 complex. It has lately been realized that HH flows may attain dimensions far beyond earlier estimates, increasing the possibility that we may witness a jet colliding with an obstruction of dense material in its path, and what appears to be such a case is discussed. Finally, the role of both infrared imaging and spectroscopy for HH research is outlined.

Key words: **ISM: JETS AND OUTFLOWS — STARS: FORMATION**

1. INTRODUCTION

In the almost half century during which we have known of Herbig-Haro objects, our perception of them have changed dramatically. From being small peculiar nebulae found in regions of young stars, they are now seen as essential elements in the processes required to form a star out of a molecular cloud. It is also becoming increasingly clear that they play a fundamental role in driving the ubiquitous molecular outflows that escavate newborn stars from their placental material. And we are getting tantalizing glimpses of how different spectral characteristics of young low-mass stars can be understood in terms of accretion events, that may ultimately power the mass loss from these stars. But the actual mechanism of jet formation is still shrouded in the dense circumstellar disks out of which jets emerge, and observations have not been able to significantly guide or constrain theoretical studies of the formation of jets.

2. THE HH 46/47 JET COMPLEX

As a way of describing what kind of observations that can successfully be done of HH jets, this section will give an overview of what we know about the HH 46/47 jet, one of the finest jets known. Complete references to the existing literature on this object is listed in the Herbig-Haro catalogue by Reipurth (1994).

The two HH objects, HH 46 and HH 47, were discovered by Schwartz (1977). They are associated with a cometary globule in the Gum Nebula (Bok 1978), which harbours a deeply embedded infrared source (e.g. Cohen et al. 1984). This was the first HH jet that was recognized as such (Dopita, Schwartz, & Evans 1982). It is a bipolar HH system, with an approaching lobe containing a fine jet ending in a bright bow shock (47A) and further out a fainter, more extended bow shock (47D), and a receding lobe with a faint counter-jet and another bow shock (47C) (Dopita, Schwartz, & Evans 1982, Graham & Elias 1983). Proper motion studies show the two lobes moving away from the source (Schwartz, Jones, & Sirk 1984, Eislöffel & Mundt 1994). The structure of the approaching lobe as seen in a logarithmic contour plot of the sum of Hα and [SII] images is shown in Fig. 1, from Hartigan et al. (1993).

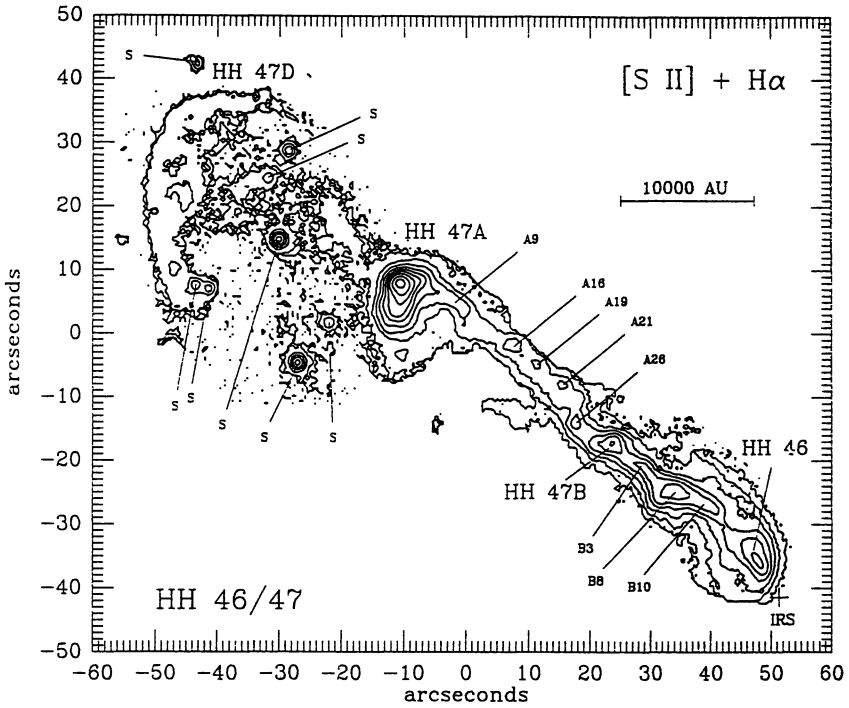

Fig. 1.— The HH 46/47 jet complex seen in a logarithmic contour plot of the sum of the [SII] 6717/6731 and Hα lines. North is up and east is left. The scale bar assumes a distance of 450 pc. Stars are marked with an "S". From Hartigan et al. (1993).

The rich emission-line spectrum of the HH 46/47 complex allows a number of physical parameters of the flow to be determined. Fig. 2 shows a low-dispersion spectrum of HH 47A, from Morse et al. (1994), which demonstrates that it is a low excitation object, with prominent lines of [SII], [OI] and [NI] and other low excitation lines (e.g. Dopita 1978, Morse et al. 1994). The electron density n_e can be derived at any point of the flow from the ratio of the [SII] 6717 and 6731 lines, and the spatial distribution of the electron density along the flow can be traced with long slit high resolution spectroscopy (e.g. Meaburn & Dyson 1987). More recently, Morse et al. (1994) have shown the great advantage of using a Fabry-Perot interferometer to observe HH jets. Such observations allow the simultaneous determination of the electron density (at specific velocities or integrated over the linewidth), the excitation level as measured by the [SII]/Hα ratio, and the detailed velocity field of the flow. The electron densities in the HH 46/47 complex has a large range, between about 30 to more than 2000 cm^{-3}. The largest values are found at the base of the jet in HH 46, similar to what is found in other jets like HH 34, HH 83 and HH 111. Another point of high density is at the apex of the HH 47A bow shock.

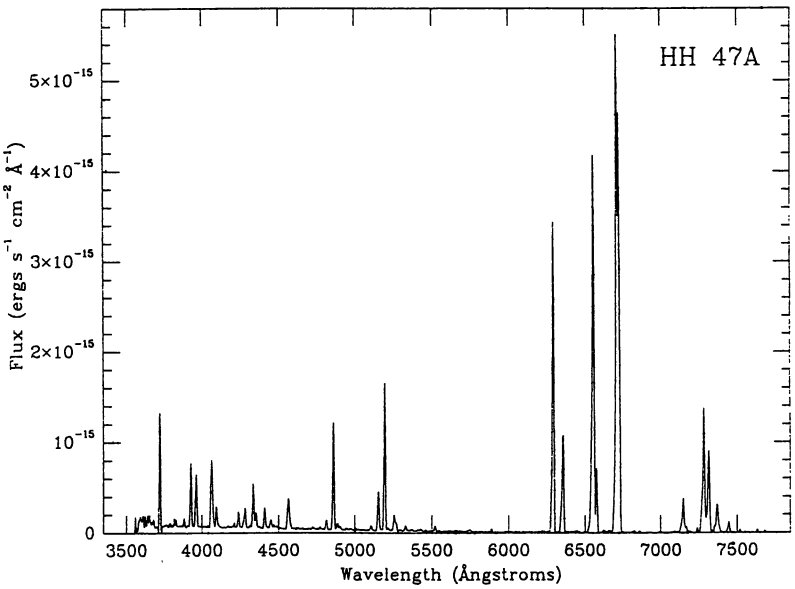

Fig. 2.— A flux-calibrated low-resolution spectrum of HH 47A. Note the weak blue continuum, which is due to two-photon emission at the apex of the bow shock. From Morse et al. (1994).

The HH 46/47 jet complex contains at least 3 working surfaces: 47A, 47D and 47C, and possibly a fourth, 47B. As seen in Figure 1, 47D is a large bow shaped feature. It is strong in Hα and weak in [SII], that is, a high excitation object. Exactly opposite and symmetrically located about the embedded source is 47C, a working surface in the receding part of the flow. 47A is the brightest region in the entire flow. It does not have a counter part in the receding lobe, possibly due to the much heavier extinction there.

As in any two fluids that collide supersonically, two shocks occur when a supersonic jet rams through its ambient medium: a shock in which environmental material is accelerated, called the bow shock, and a shock in which the jet material is decelerated, called the Mach disk. Using interference filter images obtained in excellent seeing, Reipurth & Heathcote (1991) were able to separate these two shocks. They find that HH 47A is stronger in [SII] than in Hα all over except in a narrow Hα dominated region perpendicular to the jet axis, located where the jet enters the working surface. In other words, the Mach disk has a higher excitation spectrum than the bow shock, and consequently is a stronger shock. The condition of ram pressure balance across the working surface requires that the Mach disk will be stronger than the bow shock in a jet which is less dense than the ambient medium, and conversely for a heavy jet (Hartigan 1989). Thus the observations imply that HH 47A moves into a medium with higher density than in the jet, which at first seems surprising. But HH 47A moves into a medium already shocked by and set in motion by the passage of an earlier bow shock, HH 47D, as first suggested by Dopita (1978). Gas passing through a radiative shock like HH 47D will be accelerated to a velocity only slightly less than that of the working surface. A co-moving ambient medium will also weaken the shocks in the HH 47A working surface, so that a high space motion combines with a low shock velocity, as expected from its low excitation character. Additionally, the wake of HH 47D, into which HH 47A moves, consists of both ambient gas and jet gas, both of which have been compressed in the HH 47D working surface, thus explaining the denser medium found ahead of HH 47A.

The Fabry-Perot data of Morse et al. (1994) allows a kinematic separation of the bow shock and Mach disk. Combining the available spectroscopic and kinematic data they estimate a shock velocity for the apex of HH 47A of about 60 km s^{-1}.

HH 47D can also be separated into a bow shock and a Mach disk (Hartigan et al. 1990, Reipurth & Heathcote 1991). Morse et al. (1994) kinematically isolated the two shocks, and also here find that the shock velocity is much lower than the space velocity as derived from radial velocity and proper motion measurements. Thus also HH 47D is following in the wake of previously ejected material.

As a jet propagates through its ambient medium, it interacts with this medium and slows down while

accelerating its surroundings. This is discussed in more detail in the following section and in the review of Raga (1995) in these Proceedings. In the HH 46/47 jet there is kinematic evidence for entrainment of material along the body of the jet, first recognized in the high-resolution long-slit spectra of Meaburn & Dyson (1987). The Fabry-Perot data discussed by Hartigan et al. (1993) and further analyzed by Raymond et al. (1994) allow a subtraction of high- and low-velocity emission. It is very clear that the high-velocity gas is surrounded by low-velocity material, in other words the flow moves faster along the middle of the jet than at the edges, similar to a viscous flow in a pipe. High excitation emission is also found to occur along the edges of the jet, which is what one would expect if the entrainment process accelerates and heats the ambient material.

The HH 46/47 jet coincides with a weak molecular outflow, with a short blue lobe where the jet breaks out of the globule, and a more extended red lobe where the jet burrows through the top of the globule, eventually to break free on the opposite side and emerge as the HH 47C bow shock (Chernin & Masson 1991, Olberg, Reipurth, & Booth 1992). This flow may be ambient material set in motion by the passage of the jet. Infrared molecular hydrogen observations have revealed the outline of the red flow cavity, which is lined by weak H_2 emission (Eislöffel et al. 1994).

The evidence for multiple bow shocks in the HH 46/47 flow is not isolated, indeed it is a common feature of the best collimated jets, like HH 111 and HH 34. This has been interpreted as the result of multiple FU Orionis like disk accretion events in the driving source (Dopita 1978, Reipurth 1989). Using the known space velocities of the working surfaces, the age of HH 47B, A and D are of the order of 500, 1100 and 1800 yr. These numbers are obviously very uncertain, based as they are on an assumption of constant flow velocity and on limited data, but they point, like for other jets, towards major eruptions in the source every many hundred years. Individual knots in the jet may be due to more frequent but smaller puffs from the source. Raga et al. (1990) have modelled the time evolution of a train of multiple working surfaces, with particular reference to the HH 46/47 flow.

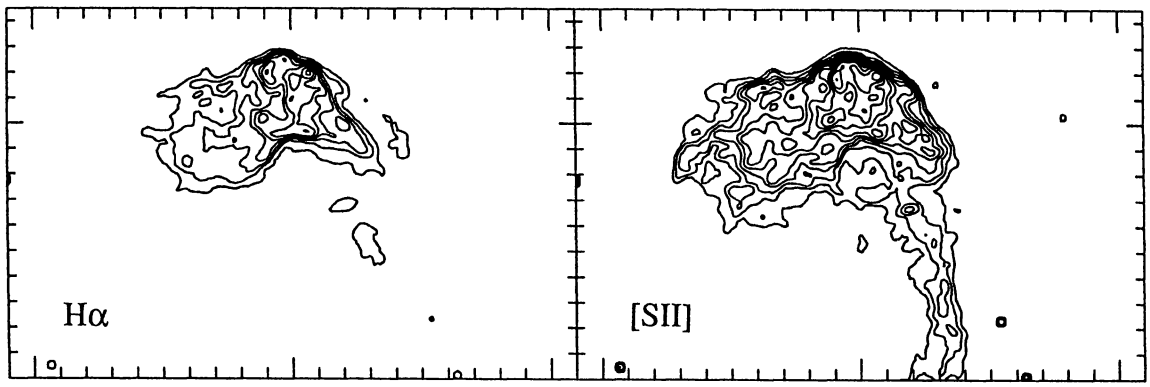

Fig. 3.— The HH 47A working surface as seen in CCD images obtained by HST through Hα and [SII] filters. From Heathcote et al. (in preparation).

There is a large reflection nebula at the base of the jet, illuminated by the embedded source. This acts as a mirror that permits us to obtain information on the driving source. The reflection nebula is highly variable, probably as a result of material moving close to the star (Graham 1987, Reipurth & Heathcote 1991). Optical spectra of the nebula reveal a rich emission line T Tauri spectrum (Graham & Heyer 1989, Reipurth & Heathcote 1991). The star is thus presently in a stage in between FU Orionis eruptions.

The HH 46/47 complex has recently been observed with the Hubble Space Telescope through Hα and [SII] interference filters using WFPC2 (Heathcote et al., in preparation). The jet shows up in splendid detail in these unprecedented views, and with a pixel size of 0.1 arcsec it is everywhere fully resolved. However, at the time of writing the data are still in the process of being analyzed. HH 47A, the most prominent working surface in the flow, is seen in Fig. 3 in both Hα and [SII]. The low-excitation jet is seen to curve into the working surface at an angle and ends in the Mach disk, which is seen in the Hα image as a thin horizontal feature. The bow shock is very wide and asymmetric, as if the flow has a sideways motion because of the slanted injection angle of the jet. The front of the bow shock is clearly strongly compressed, with a steep emission gradient. Interior to this it turns out that the bow shock is very inhomogeneous, consisting of a myriad of tiny irregular structures. A full analysis will be presented by Heathcote et al. (in preparation).

3. THE RELATIONSHIP BETWEEN HH JETS AND MOLECULAR OUTFLOWS

Molecular outflows are found in all active star forming regions and importantly influence their surroundings (see Bachiller & Gómez-González 1992). In a number of cases Herbig-Haro objects are found to co-exist with molecular outflows, but in most cases when one of the two types of flows is found the other is not. The precise relation between the two phenomena is currently a subject of much research.

A number of theoretical works have suggested that an HH jet as it moves through the ambient medium entrains material and thus transports momentum to the surrounding molecular cloud. This gradually would set more and more of the cloud material into motion, which may be observed as a molecular outflow.

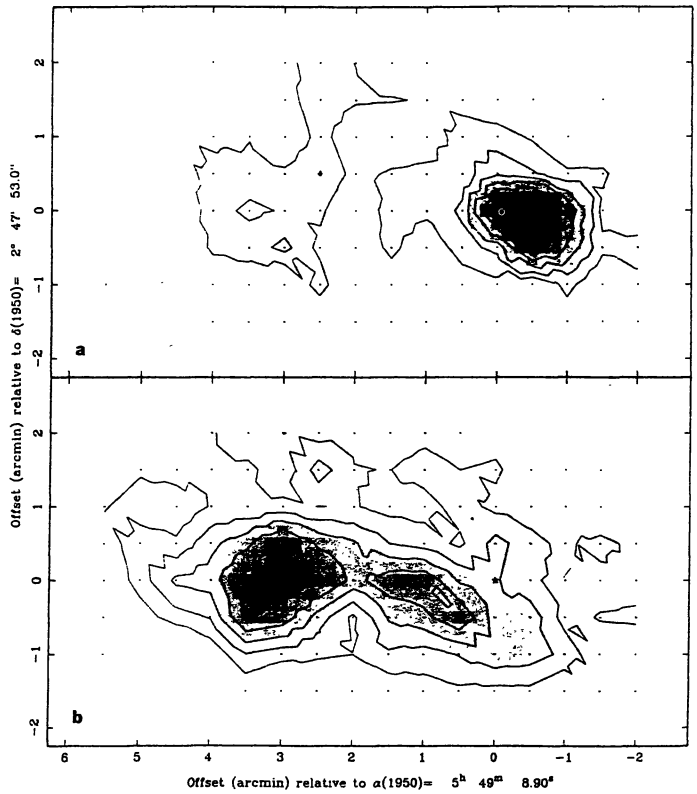

Fig. 4.— The molecular outflow surrounding the HH 111 jet complex. Panel A shows the blueshifted ^{12}CO emission and panel B the red shifted ^{12}CO emission. The asterisk denotes the position of the energy source. From Reipurth & Olberg (1991).

The models have principally focused either on what happens when a bow shock sweeps up ambient material and releases it in a turbulent wake, or the results of the formation of a turbulent mixing layer along the body of the jet.

The first concept has been explored analytically by Raga & Cabrit (1993) and Masson & Chernin (1993), the former dealing with an internal working surface, and the latter with a leading working surface. Seen in a frame moving with the working surface, material enters the region between the two working surface shocks from both sides of the flow axis, and is ejected sideways, where it interacts with the ambient material that is streaming by. This results in a bow shaped contact discontinuity where shocked jet material blends with ambient material in a turbulent mixing layer. In the Raga/Cabrit model this hot dense layer expands and fills in the cavity behind the working surface, forming a turbulent wake which may be observable as a molecular outflow. Masson and Chernin interpret the swept up shell as the molecular outflow. Raga et al. (1993) have considered the integrated effect of many internal working surfaces, and find that it leads to the formation of a large turbulent envelope, which can be associated with a molecular outflow.

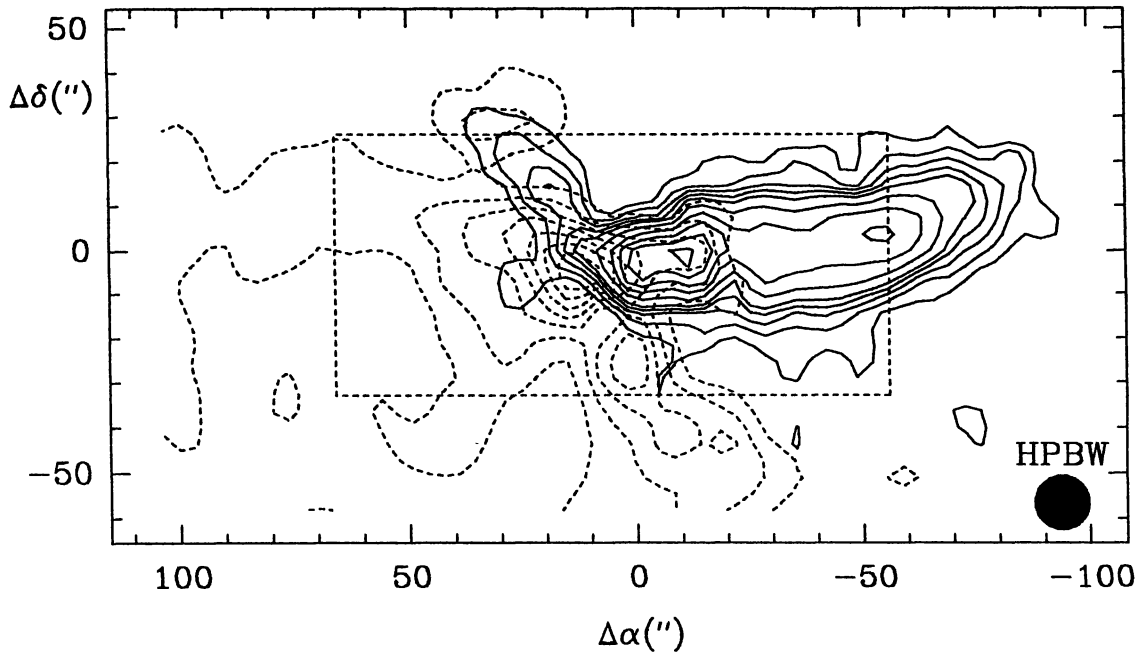

Fig. 5.— The blue and red lobes of the HH 111 molecular outflow observed in ^{12}CO (2-1) with the IRAM 30m telescope. The FWHP beamwidth is 12 arcsec and the spacing of the observations 7 arcsec. The dotted box outlines the area shown in Fig. 6. From Cernicharo & Reipurth (1995).

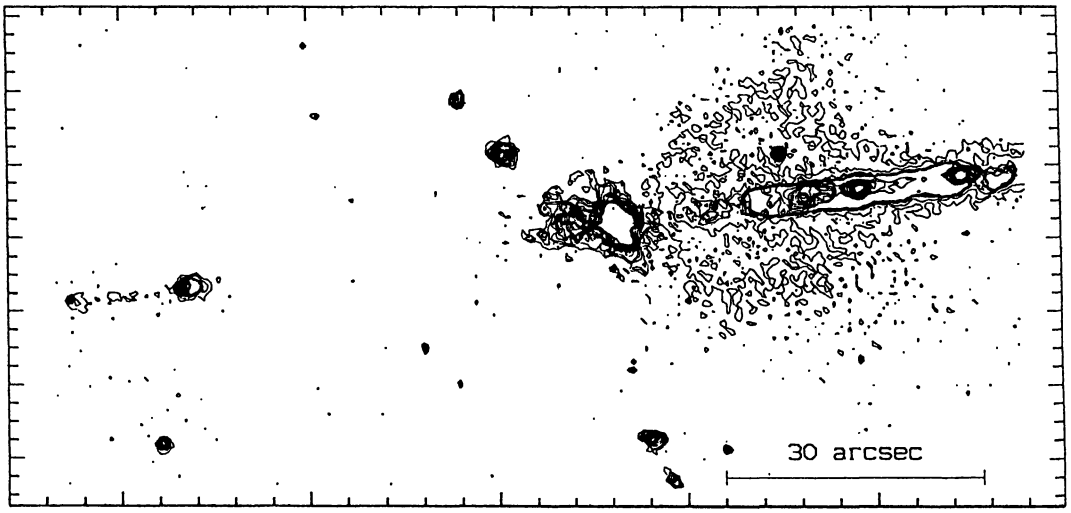

Fig. 6.— A composite of an optical [SII] image and an infrared H_2 image. A compact infrared reflection is located at the apex of the large fan-shaped optical reflection nebulosity. The deeply embedded VLA source that drives the jet is situated 5″ east of the IR reflection nebula. From Gredel & Reipurth (1994).

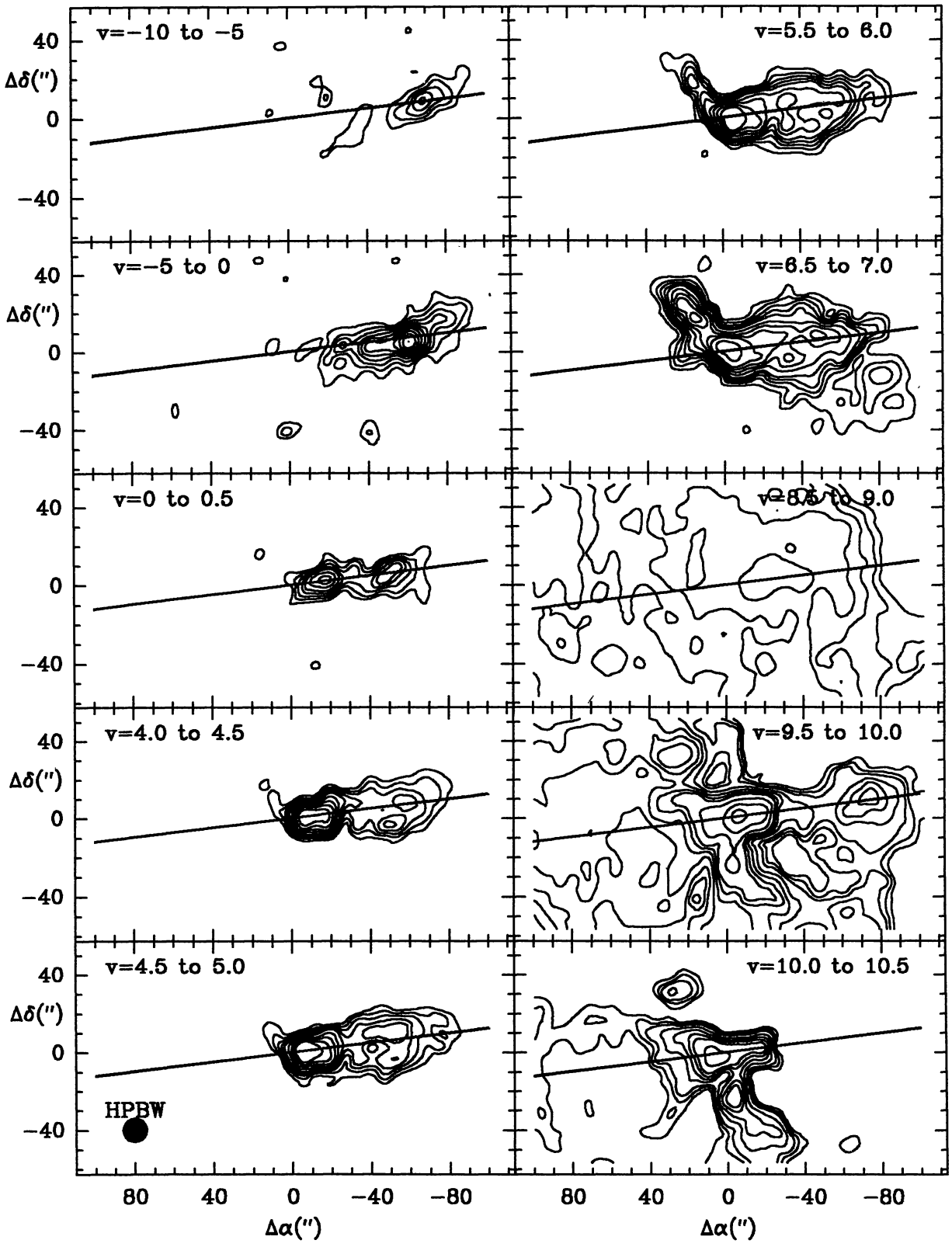

Fig. 7.— A mosaic of 10 individual velocity-channel maps of the HH 111 molecular outflow observed in ^{12}CO (2-1) with the IRAM 30m telescope. From Cernicharo & Reipurth (1995).

The second concept is based on a view of an HH jet as a highly supersonic, uniform, pressure matched beam moving through the surrounding environment. Cantó & Raga (1991) described the properties of the turbulent mixing layer that is formed between the two fluids, when the jet is uniform and the environment is stationary. Raga, Cabrit, & Cantó (1995) extended this work to describe the mixing layers between two moving, inhomogeneous media. The lateral entrainment that occurs at the jet/environment boundary may drive the molecular outflows. Stahler (1994) has compared this concept with observations of molecular outflows. Most recently, Taylor & Raga (1995) have incorporated a detailed treatment of the chemical properties of a mixture of atomic jet material with molecular environmental material, in particular giving predictions of the expected H_2 emission line spectrum.

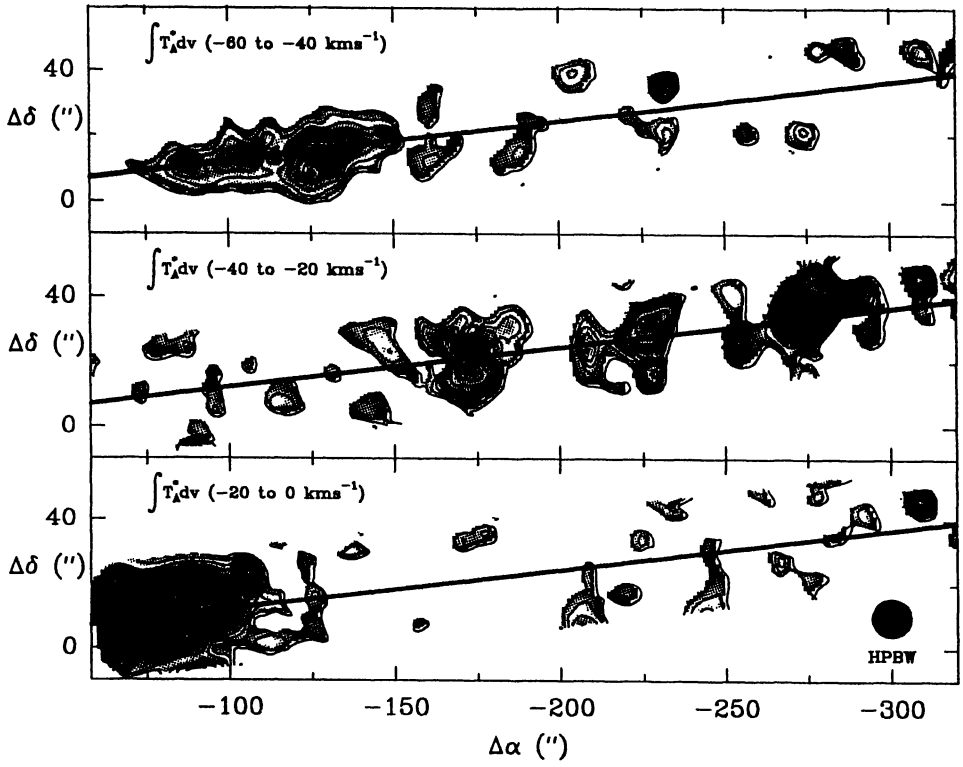

Fig. 8.— Three velocity maps of the region 5 arcmin west of the HH 111 energy source. High velocity bullets along the jet axis are seen in the middle panel. From Cernicharo & Reipurth (1995).

Two of the finest HH jets known, HH 46/47 and HH 111, have been found to drive molecular outflows. The first of these regions was discussed in Section 2. Mm line observations have been done of the HH 111 region by Reipurth & Olberg (1991), who discovered a major molecular outflow along the HH jet axis. Fig. 4 shows the blueshifted and redshifted ^{12}CO emission along the HH 111 jet axis. The asterisk indicates the location of the driving source. The principal part of the optically visible jet complex moves abruptly out of the cloud core into essentially empty space. This is because the UV radiation from the OB stars in the Orion Ib association has destroyed the less dense material that would normally surround a dense cloud core. As expected in such an environment, the blue lobe of the molecular outflow along the HH jet is very short, whereas the red lobe where the HH flow is partly buried in the surrounding molecular cloud is long and massive.

The HH 111 molecular outflow has been observed with higher spatial resolution (FWHP $\approx$ 12 arcsec) in the ^{12}CO (2-1) transition at the IRAM 30m telescope (Cernicharo & Reipurth 1995). Fig. 5 shows a composite of the blue and red ^{12}CO lobes in the inner part of the outflow; the red wing is integrated between +10.0 and +16.5 kms^{-1} and the blue wing between −5.0 and +7.0 kms^{-1}, and the cloud velocity is around +8.5 kms^{-1}. The source is located at (0,0). It is obvious from the figure that the blue lobe is remarkably collimated, while the red lobe is more stubby and appears to open up. The rectangular box in the center of the map corresponds to the size of Fig. 6, which shows a composite of optical and infrared images of the jet complex, from Gredel & Reipurth (1994). It clearly illustrates that the Herbig-Haro jet is perfectly aligned with the central part of

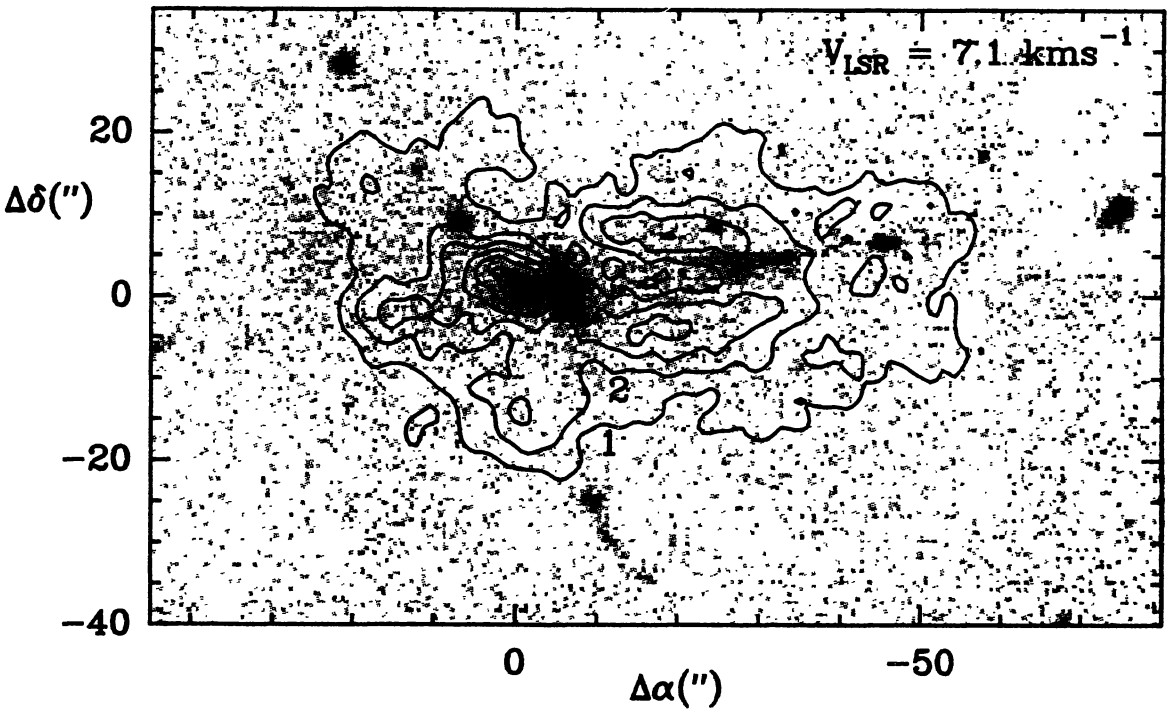

Fig. 9.— The HH 111 molecular outflow at HH 111 at a velocity of +7.1 kms^{-1} as observed with the Plateau de Bure Interferometer with a beam of 2″ x 3″. The contour plot is overlaid on an H_2 image obtained by J. Eislöffel. From Cernicharo et al. (in preparation).

the molecular jet. Fig. 6 also shows the presence of a second bipolar HH flow, HH 121, detected only in the infrared and emanating almost perpendicular to the main jet axis (Gredel & Reipurth 1993). The detailed mm observations show that also this smaller HH flow drives its own molecular flow, so that the whole system is quadrupolar. A series of 10 individual velocity-channel maps is presented in Fig. 7. In the blueshifted frames it is apparent that the molecular outflow displays the well known "acceleration" effect, seen also in a number of other molecular outflows. The peak intensity of each of the channel maps moves closer to the source as the velocity approaches that of the cloud, until the peak is centered on the VLA source just before the flow blends with the ambient cloud. A similar but less pronounced effect is noted in the shorter red lobe. It is also evident that there are several clumps in the outflow. Furthermore, in particular in the blue lobe of HH 111 one can see a two-component velocity structure, with the blue lobe showing up again in the +9.5 to +10.0 kms^{-1} map.

The well defined blue lobe of the HH 111 molecular outflow ends about 90 arcsec from the source. But this is not the end of the molecular outflow. Fig. 8 shows three channel maps of the region five arcminutes west of the source, integrating the velocities from −20 to 0 kms^{-1}, −40 to −20 kms^{-1}, and −60 to −40 kms^{-1}. The molecular outflow around the jet is seen in the lower panel. A very high velocity and very well collimated extension of the jet out to 150 arcsec from the source is apparent in the upper panel. But the big surprise is the presence of three high velocity bullets in the middle panel. These three bullets are located precisely on the axis of the Herbig-haro jet, at distances of 170, 220 and 270 arcsec from the source, corresponding to 0.38, 0.49 and 0.60 pc in projection. If these bullets lie at the same angle of 10° to the plane of the sky as the Herbig-Haro jet (Reipurth, Raga, & Heathcote 1992), then they have space velocities in excess of 200 kms^{-1}. Their ages are thus of the order of 1700, 2200 and 2700 yr. This regular spacing suggests that they result from eruptions in the driving source which occurred with intervals of about 500 yr.

The inner part of the HH 111 molecular outflow has recently been mapped with the Plateau de Bure Interferometer with a resolution of 2″ x 3″ (Cernicharo et al., in preparation). Fig. 9 shows the molecular outflow at the velocity of +7.1 kms^{-1}, overlaid on an H_2 image by J. Eislöffel. While the detailed analysis of the data is still being carried out at the time of writing, the principal results is obvious from the figure: the inner part of the molecular outflow consists of two lobes on either side of the Herbig-Haro jet. This is exactly what

one would expect from the limb-brightened edges of a tube of gas surrounding a jet. These observations for the first time provide direct observational evidence for the theoretical ideas that Herbig-haro jets are powering the molecular outflows. The width of the tube is 11 arcsec, corresponding to 5000 AU at a distance of 460 pc. It is noteworthy that the width of the principal bow shock V in the HH 111 jet complex is 8 arcseconds. These dimensions suggest that the principal interaction between the jet and its ambient medium is not along its body (which has a width of 0.8 arcsec), but rather along the edges of the multiple bow shocks that are shooting out from the star.

Far from all Herbig-Haro jets drive molecular outflows. A case in point is the HH 34 jet, which shares many properties with the HH 111 jet. Reipurth et al. (1986) searched in vain for a molecular outflow at HH 34, and only recently have new sensitive observations of Chernin & Masson (1995) revealed a very weak and small molecular outflow. The difference between the molecular outflows of these two jets may be one of their environment, but could also be evolutionary, with the HH 111 energy source being younger than the source of HH 34, and so the HH 34 flow has had more time to evacuate material from its surroundings.

4. THE DIMENSIONS OF HERBIG-HARO FLOWS

The HH 46/47 jet complex has two equally large lobes, each with projected dimensions of 0.28 pc at the assumed distance of 450 pc. as it turns out this is a farly typical size of a Herbig-Haro flow from a low luminosity star. The HH 34 jet complex, as another example, has two symmetric lobes, each 0.25 pc long and ending in the working surfaces HH 34 and HH 34-North.

Possibly because so many flows have similar dimensions or are even smaller, it came as a major surprise when Bally & Devine (1994) presented evidence that the HH 34 complex is in fact six times larger, with a total projected extent of almost 3 pc. The HH 34 jet complex is located in a region of the L1641 cloud in Orion which is rich in young stars and HH objects. North of the HH 34-North bow shock one finds the well known bright HH objects HH 33 and HH 40, in addition to HH 85 and HH 126. South of HH 34 there is HH 86, HH 87 and HH 88 as well as the faint HH 173. For none of these objects were a plausible energy source ever found. Bally & Devine (1994) realized that all these objects lie very close to the well defined axis of the HH 34 jet (see Fig. 10, Plate 1). Moreover, for those objects for which kinematic data are available it turns out that all HH emission south of HH 34 IRS is blueshifted, whereas all HH objects north of the source are redshifted (Bally, priv. communication). This is very strong evidence in favor of the view that all of these objects are in fact a single giant HH flow. A proper motion study is presently being carried out to further test this model.

Two other very large HH complexes are known, the Z CMa flow with a projected extent of 3.6 pc (Poetzel, Mundt, & Ray 1989) and the HH 80/81 flow that stretches over about 5.6 pc (Martí, Rodríguez, & Reipurth 1993). But in both these cases the sources driving the flows are high-luminosity stars of either medium or high mass.

It is perhaps noteworthy that the area of the sky covered by what is currently a typical CCD detector (say, 1000 x 1000 pixels of about 0.4 arcsec each) is between 0.3 x 0.3 pc to 1 x 1 pc in star forming regions at distances between Taurus and Orion. It shall be interesting to see if the typical sizes of HH flows grow as our detectors continue to grow.

5. HH JETS COLLIDING WITH MOLECULAR CLOUD CORES

With the realization that HH flows can be much larger than previously anticipated, comes the question whether such large jets are likely to find an obstacle-free path stretching over several parsecs. Given that the molecular clouds out of which jets emerge are often large and have complex structure with cloud cores, the answer is probably that large jets may well from time to time collide with dense regions in their surroundings. An example of what appears to be precisely such a case has very recently been identified.

Fig. 11 shows a contour plot from an Hα image of the HH 110 flow. It is a major HH flow consisting of many knots embedded in a matrix of low-level emission and stretching over 3 1/2 arcminutes, which at the distance of the L1617 cloud in Orion (460 pc) corresponds to 0.45 pc (Reipurth & Olberg 1991). Although the jet is initially well collimated, it soon widens in a cone with an exceptionally large opening angle of 12°. At the same time it appears that oscillations are set up, which end in large graceful curves as the flow fades to invisibility. Although a number of jets are known to show wiggles, this may well be the finest case.

From the morphology one would expect the energy source to be located very close to the apex of the flow. However, there is no source in the IRAS catalogue at that position, and deep searches at near-infrared as well

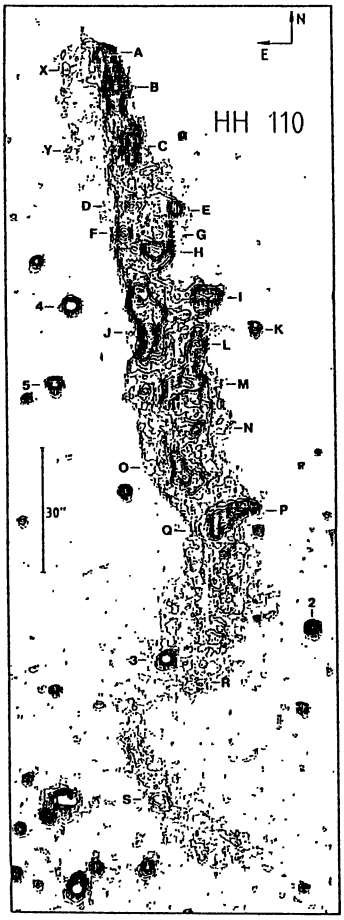

Fig. 11.— A contour plot of an Hα image of the HH 110 flow. North is up and east is left. From Reipurth & Olberg (1991).

as at sub-mm and cm wavelengths have not uncovered a source. This is highly unusual, since virtually all well collimated flows, thanks to their geometry, have well identified energy sources.

In a recent study Reipurth, Raga, & Heathcote (1995) obtained large field interference filter CCD images of the HH 110 region, and discovered a faint new HH flow, HH 270, about 2 1/2 arcminutes to the north-east of HH 110. Fig. 11 shows a contour plot from an Hα CCD image of HH 270. Five knots, A to E, are identified, and knot A, which is the leading knot in the flow, has the morphology of a tiny bow shock. To the east of knot E there is a dark lane, and east of that a very faint pencil of light. This latter feature is probably a beam of light escaping from a deeply embedded source located in the dark lane, where a faint nebulous infrared source has been detected. HH 270 is seen to be located in a dark cloud with a well defined edge bordering to the south to a region of weak Hα emission.

HH 270 lies along a position angle of about 261°, almost directly pointing towards the apex of HH 110, seen to the lower right of Figure 12. As it turns out, HH 270 knot A was fortuitously included in an image obtained 6 years earlier, from which it has been possible to derive the proper motion of that knot. It is found to move with a tangential velocity of 300 km s^{-1} along a vector pointing directly towards HH 110 knot A, the apex of this flow. The knots in HH 110 itself, on the other hand, all move in more or less the direction defined by the flow axis of the HH object.

The absence of an energy source for HH 110 and the morphology and kinematics of HH 270 led Reipurth, Raga & Heathcote (1995) to suggest that the HH 110 jet is the result of the HH 270 flow suffering a grazing collision with an obstruction in the molecular cloud from which HH 110 is seen to emanate. The result of the

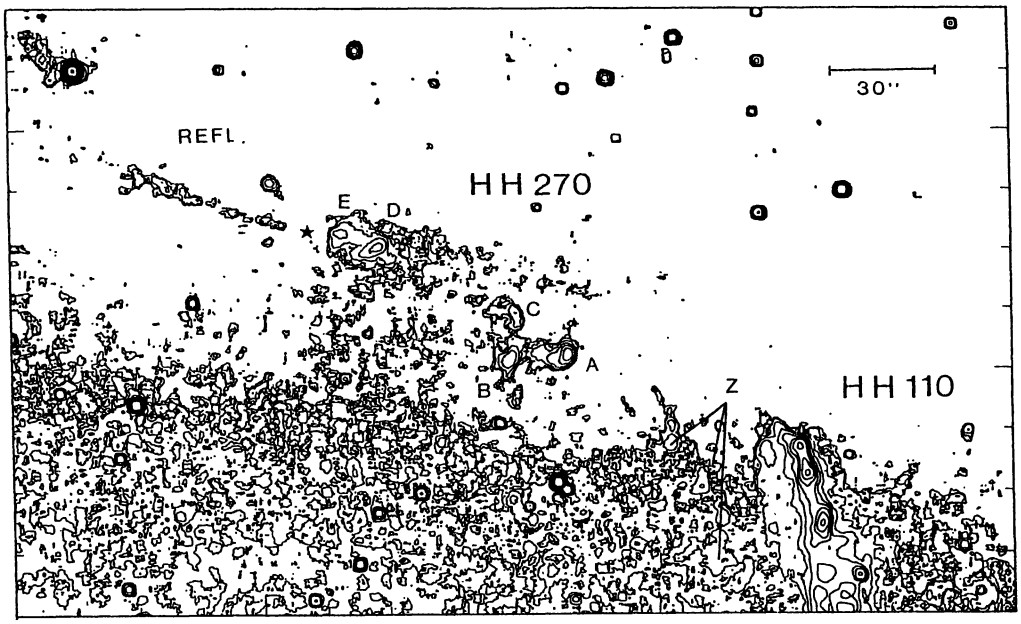

Fig. 12.— A region of approximately 3′ x 4.5′ around the beginning of the HH 110 flow. A new flow, HH 270, is indicated. The asterisk marks the position of the embedded driving source. North is up and east is left. From Reipurth, Raga, & Heathcote (1995).

collision is that the high velocity gas in the HH 270 flow, which is only partly shocked, goes through a shock while being deflected, and emerges as the complex HH 110 flow.

In order for the HH 270 flow to be deflected, it must encounter something dense in its flow-path. Millimeter observations have revealed two molecular cores in the region; one is centered on HH 270 IRS and the other is located just north-west of the apex of HH 110, indeed where one would expect the required density enhancement. It is perhaps noteworthy that a very young star driving a major molecular outflow is embedded at the center of this latter cloud core. The larger question arises if the jets from a young star in one core can push another neighboring core over the threshold of collapse.

Analytical studies of the deflection of a jet shows that the outgoing beam is slowed by a factor $\cos\theta$ compared to the incoming jet, where θ is the angle of deflection (Cantó et al. 1988). Assuming that the HH 270 and HH 110 flows lie close to the plane of the sky, and using the proper motions of the knots in the two flows and the abovementioned relation, one predicts a deflection angle of about 62°. This compares favorably with the observed projected deflection angle of 58°. While the uncertainties involved are such that this fine correspondence is almost certainly fortuitous, it does lend credence to the interpretation of HH 110 as a deflected HH flow.

In the review by Raga (1995) the theoretical background for a flow being deflected at a density enhancement is further discussed.

6. MOLECULAR HYDROGEN OBSERVATIONS OF HH FLOWS

Near-infrared imagers and spectrographs have now reached such a level of development that it is possible to study the morphology and line strengths of the infrared emission from a large number of HH flows, particularly the strong and abundant infrared lines of H_2, the strongest of which is the (1,0) S(1) line at 2.12 μm. Additionally, spectra in the H-band will record the [FeII] lines at 1.64 μm and 1.25 μm, which both arise from the same upper level, and therefore can be used to derive the reddening in an HH flow. [FeII] lines are also useful indicators of electron density.

The ground state of H_2 has many vibration-rotation levels with excitation energies from less than 1000 K

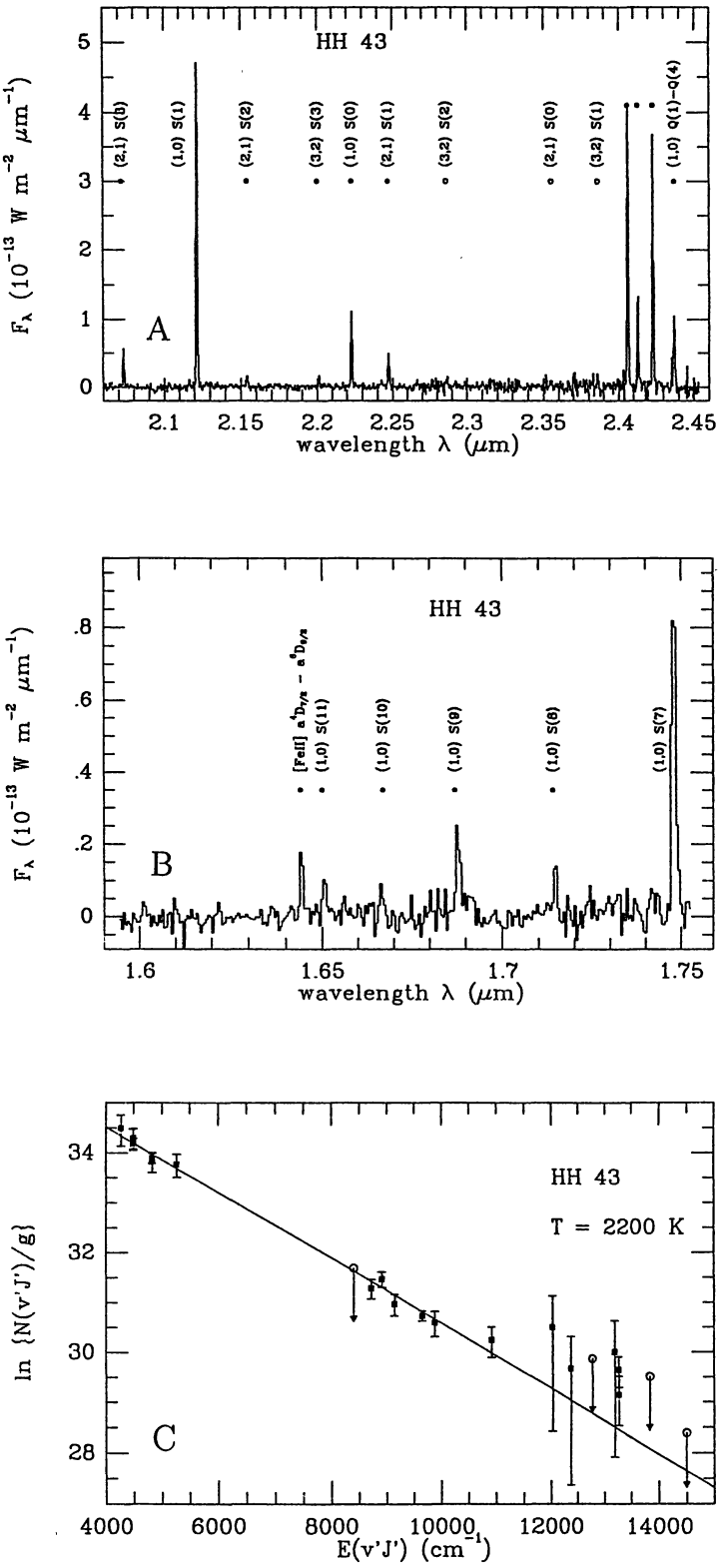

Fig. 13.— Infrared spectroscopy of HH 43. Panel A shows a K-band spectrum, and Panel B an H-band spectrum. Panel C shows the resulting H_2 excitation diagram. From Gredel (1994).

to several 10000 K. The resulting lines are likely to be collisionally excited in shocked gas with temperatures of a few thousand degrees, as originally discussed by Elias (1980). Such thermal excitation will populate only the lowest vibrational levels (v≤3). Other non-thermal mechanisms have been discussed as well, particularly excitation due to fluorescence pumped by UV photons. Such processes will populate also high (v>3) vibrational levels. High signal-to-noise spectra of spectral regions where higher vibrational level lines should appear are therefore important in order to distinguish between thermal and non-thermal excitation mechanisms.

A convenient way of presenting the information of molecular hydrogen spectra is the H_2 excitation diagram, in which a measure of population density is plotted against excitation energy of the upper level for each transition. Gredel (1994) discusses the underlying physics, here it suffices to say that if the emitting gas can be characterized by a single temperature then the data points will fall along a straight line, with a slope proportional to the inverse of the excitation temperature. If, on the other hand, the emission comes from gas at a range of temperatures, then the line will be curved.

High resolution long-slit near-infrared spectra were obtained along the body of the HH 111 jet by Gredel & Reipurth (1993). The excitation diagram shows that the gas in the principal knots detected is thermalized at a constant temperature of 2150±400 K. Although the HH 111 jet is not especially bright in H_2 it is at least rather easily detectable. On the other hand, the HH 34 jet, which optically appears almost as a twin to the HH 111 jet, has not been detected so far in H_2 (Stapelfeldt et al. 1991). No explanation has as yet been found for this surprising difference between apparently similar jets, which may reflect our still rudimentary understanding of molecular emission in shocks. Of course it could also simply be that the much stronger molecular outflow at HH 111 as compared to HH 34 (see Section 3) provides an abundant supply of ambient molecular hydrogen not found in HH 34.

Gredel (1994) has obtained high resolution spectra of a large number of HH flows. For all of the objects, he finds a thermal population distribution which can be described by single excitation temperatures in the range from 2000 K to 2700 K. Included among these objects is HH 43, which is one of the brightest H_2 emitters among HH objects. Fig. 13 shows in panel A the K-band spectrum of HH 43, in panel B the H-band spectrum, and in panel C the resulting excitation diagram. Gredel derives an excitation temperature for HH 43 of 2200 K. In the H-band spectrum there should be five (6,4) Q(1)-Q(5) lines in the 1.60 to 1.64 μm region if any non-thermal emission was present. None are seen. There *is* in fact fluorescently excited H_2 in HH 43, but it has so far only been detected in the UV, where Schwartz (1983) observed eight Lyman band emission lines between 1250 Å and 1600 Å.

Both C-type (continuous) and J-type (jump shocks) have been invoked to explain the infrared line spectra in HH flows. C-shocks require a magnetized medium of low ionization (e.g. Smith 1991, 1993). Gredel (1994) argues that such shocks are not relevant for any of the HH flows he observed, because fast C-shocks would create H_2 column-densities several orders of magnitude too large, and although slower C-shocks could give the right intensities, the corresponding excitation temperatures would then be much too low.

J-shocks require a medium of high ionization that is at most weakly magnetized (Smith 1994, 1995). The intensities in the (1,0) S(1) H_2 line that Gredel (1994) observed in various HH objects can be produced by slow non-dissociative J-shocks. The observed intensities of the [FeII] 1.64 μm line are, on the other hand, well modelled by fast, dissociative J-shocks in the 40-60 kms^{-1} range. This can be reconciled only if the H_2 and [FeII] emission originate in separate regions, and Gredel (1994) suggests that curved bow shocks of J-type could explain the data, with the [FeII] emission arising in the fast, dissociative region near the apex of the bow shock, and the H_2 emission arising in the slower, non-dissociative wings. In a new study, Schwartz et al. (1995) arrive at similar conclusions.

Clearly it is important to study differences in the spatial distribution of H_2 and [FeII]. Such studies generally find the same large-scale morphology, but with differences in the details (e.g. Stapelfeldt et al. 1991, Gredel 1994, Davis, Eislöffel, & Ray 1994). Similarly, an analysis of atomic emission and molecular emission from optical and infrared images can provide new constraints on models. Hartigan, Curiel, & Raymond (1989) compared images of HH 7 in Hα, [SII] and H_2, and suggested that a bow shock with a magnetic precursor could explain most of the observations. Indeed, the infrared Fabry-Perot images of HH 7 by Carr (1993) show that its velocity field is as expected for a radiating bow shock.

Molecular hydrogen imaging has provided some unexpected results in the discovery of optically invisible, embedded jets detected by their H_2 emission. A case is the HH 211 jet near the young cluster IC 348 in the Perseus dark cloud complex (McCaughrean, Rayner, & Zinnecker 1994). The morphology of HH 211 suggests that what we see in H_2 is the region of interaction between the jet and its surrounding medium. Coincident with the two lobes of the jet is a small molecular outflow. Thanks to the symmetry of the jet complex a deeply embedded very cool source detected only at sub-mm wavelengths was discovered between the lobes. It is

noteworthy that this very young source would not have been easily discovered if it had not been for the telltale signature of the jet.

We thank John Bally, Roland Gredel, Pat Hartigan, and Jon Morse for permission to present some of the figures accompanying this article.

REFERENCES

Bachiller, R., & Gómez-González, J. 1992, A&AR, 3, 257
Bally, J., & Devine, D. 1994, ApJ, 428, L65
Bok, B. J. 1978, PASP, 90, 489
Cantó, J., & Raga, A. C. 1991, ApJ, 372, 646
Cantó, J., Tenorio-Tagle, G., & Rózyczka, M. 1988, A&A, 192, 287
Carr, J. S. 1993, ApJ, 406,553
Cernicharo, J., & Reipurth, B. 1995, in preparation
Chernin, L.M., & Masson, C. R. 1991, ApJ 382, L93
Chernin, L. M., & Masson, C. R. 1995, ApJ, in press
Cohen, M., Schwartz, R. D., Harvey, P. M., & Wilking, B. A. 1984, ApJ, 281, 250
Davis, C. J., Eislöffel, J., & Ray, T. P. 1994, ApJ, 426, L93
Dopita, M. A. 1978, A&A, 63, 237
Dopita, M. A., Schwartz, R. D., & Evans, I. 1982, ApJ, 263, L73
Eislöffel, J., Davis, C. J., Ray, T. P., & Mundt, R. 1994, ApJ, 422, L91
Eislöffel, J., & Mundt, R. 1994, A&A, 284, 530
Elias, J. H. 1980, ApJ, 241, 728
Graham, J. A. 1987, PASP, 99, 1174
Graham, J. A., & Elias, J. H. 1983, ApJ, 272, 615
Graham, J. A., & Heyer, M. H. 1989, PASP, 101, 573
Gredel, R. 1994, A&A, 292, 580
Gredel, R., & Reipurth, B. 1993, ApJ, 407, L29
Gredel, R., & Reipurth, B. 1994, A&A, 289, L19
Hartigan, P. 1989, ApJ, 339, 987
Hartigan, P., Curiel, S., & Raymond, J. 1989, ApJ, 347, L31
Hartigan, P., Morse, J. A., Heathcote, S., & Cecil, G. 1993, ApJ, 414, L121
Hartigan, P., Raymond, J., & Meaburn, J. 1990, ApJ, 362, 624
Martí, J., Rodríguez, L. F., & Reipurth, B. 1993, ApJ, 416, 208
Masson, C. R., & Chernin, L. M. 1993, ApJ, 414, 230
McCaughrean, M., Rayner, J.T., & Zinnecker, H. 1994, ApJ, 436, L189
Meaburn, J., & Dyson, J. 1987, MNRAS, 225, 863
Morse, J. A., Hartigan, P., Heathcote, S., Raymond, J. C., Cecil, G. 1994, ApJ, 425, 738
Olberg, M., Reipurth, B., & Booth, R. S. 1992, A&A, 259, 252
Poetzel, R., Mundt, R., & Ray, T. P. 1989, A&A, 224, L13
Raga, A. 1995, in Disks, Outflows and Star Formation, ed. S. Lizano & J. M. Torrelles, RevMexAASC, 1, 103
Raga, A. C., & Cabrit, S. 1993, A&A, 278, 267
Raga, A. C., Cantó, J., Binette, L., & Calvet, N. 1990, ApJ, 364, 601
Raga, A. C., Cantó, J., Calvet, N., Rodríguez, L. F., Torrelles, J. M. 1993, A&A, 276, 539
Raymond, J. C., Morse, J. A., Hartigan, P., Curiel, S., & Heathcote, S. 1994, ApJ, 434, 232
Reipurth, B. 1989, Nature, 340, 42
Reipurth, B. 1994, in A General Catalogue of Herbig-Haro Objects, electronically published via anon.ftp to ftp.hq.eso.org, directory /pubs/Catalogs/Herbig-Haro
Reipurth, B., Bally, J., Graham , J. A., Lane, A. P., & Zealey, W. J. 1986, A&A, 164, 51
Reipurth, B., & Heathcote, S. 1991, A&A, 246, 511
Reipurth, B., & Olberg, M. 1991, A&A, 246, 535
Reipurth, B., Raga, A. C., & Heathcote, S. 1992, ApJ, 392, 145
Reipurth, B., Raga, A.C., & Heathcote, S. 1995, A&A, in press
Schwartz, R. D. 1977, ApJ, 212, L25
Schwartz, R. D. 1983, ApJ, 268, L37
Schwartz, R. D., Jones, B. F., & Sirk, M. 1984, AJ, 89, 1735

Schwartz, R. D., Schultz, A. S. B., Cohen, M., & Williams, P. M. 1995, ApJ, in press
Smith, M. D. 1991, MNRAS, 253, 175
Smith, M. D. 1993, ApJ, 406, 520
Smith, M. D. 1994, MNRAS, 266,238
Smith, M. D. 1995, A&A, in press
Stahler, S. W. 1994, ApJ, 422, 616
Stapelfeldt, K. R., Beichman, C. A., Hester, J. J., Scoville, N. Z., & Gautier, T. N. 1991, ApJ, 371, 226
Taylor, S. D., & Raga, A. C. 1995, A&A, in press

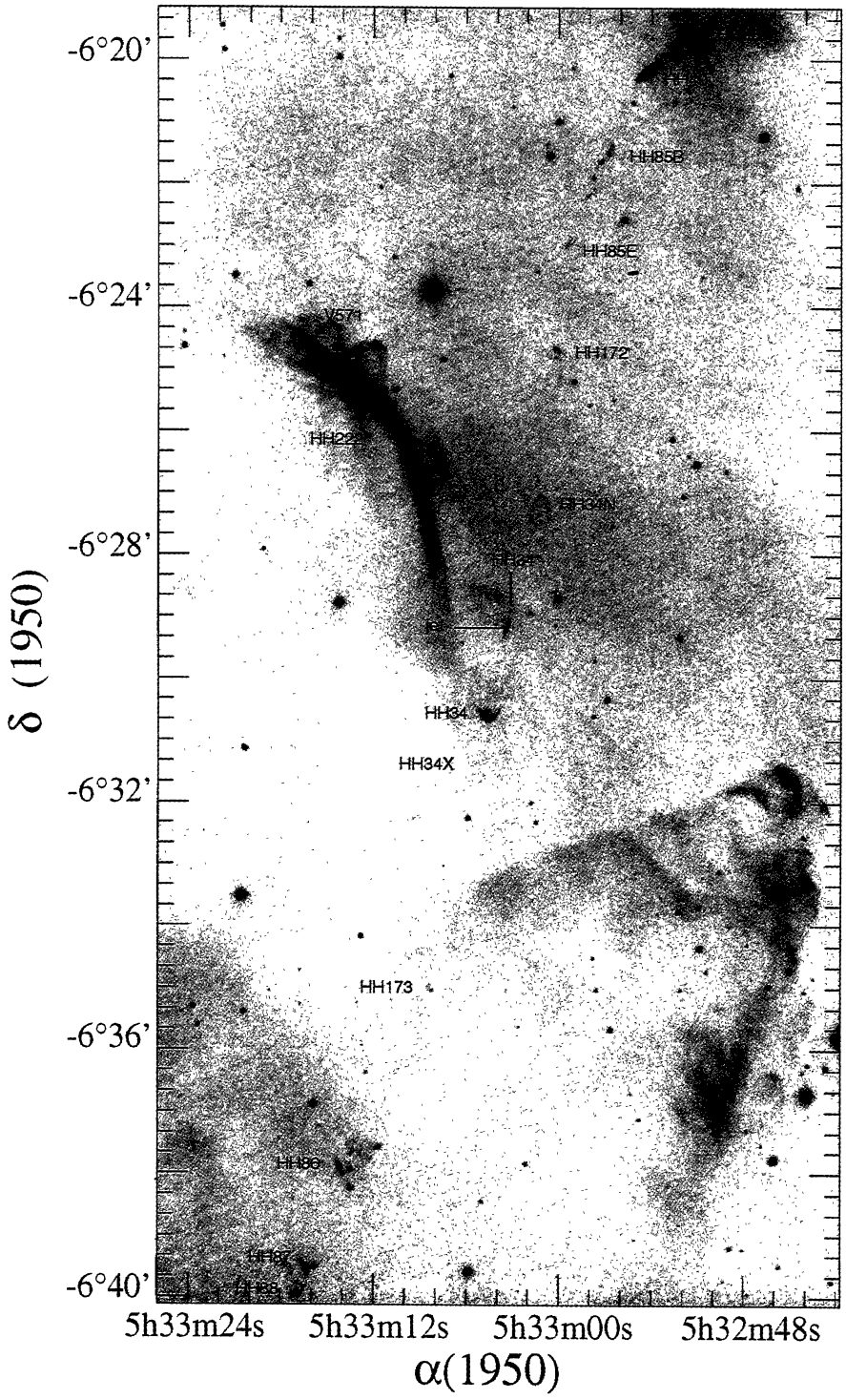

Fig. 10.— A large-field view of the HH 34 region in Hα and [SII] emission. The large chain of HH objects from HH 33 to the north-west and to HH 88 to the south-east comprises a single giant HH flow driven by the HH 34 infrared source, marked HH 34*. From Bally & Devine (1994).

REIPURTH & CERNICHARO (see page 43)